View Article Online
View Journal

Materials Horizons

Accepted Manuscript

This article can be cited before page numbers have been issued, to do this please use: S. Das, R. Singh, A. Das, S. Bag, R. P. Paily and U. Manna, *Mater. Horiz.*, 2021, DOI: 10.1039/D1MH01071A.

ROYAL SOCIETY OF CHEMISTRY

rsc.li/materials-horizons

View Article Online
DOI: 10.1039/D1MH01071A

We introduced an unconventional design of a chemically reactive conductive ink for developing non-stretchable conductive interface to identify various (slow, fast, weak and strong) human motions both in air and under water—with exceptionally high sensitivity (gauge factor ~18,300) at low applied strain. In general, highly stretchable and conductive interfaces with an well-organized surface topography are prepared to achieve high sensitivity—however such interfaces are susceptible to suffer from some unavoidable and unwanted challenges—like repetitive large tensile deformation-induced fatigue, inappropriate attachment with the human skin, water spillage accidents etc. Here, a readily amine reactive conductive ink that developed following 1,4-conjugate addition reaction between amine and acrylate at ambient condition is strategically extended for fabricating conductive and chemically reactive pattern interface—which became extremely water repellent after an appropriate post-covalent modification. On the other side, the spatially selective deposition of the prepared ink provided a facile basis for achieving ultrahigh sensitivity. Additionally, the embedded durable superhydrophobicity enabled such interface to perform—even in the presence of continuous aqueous exposure. Such an unconventional design of chemically reactive and conductive pattern interface would open up various opportunities related to healthcare, human-machine interaction, energy harvesting, etc.

Journal Name

View Article Online
DOI: 10.1039/D1MH01071A

COMMUNICATION

Abrasion Tolerant, Non-Stretchable and Super-Water-Repellent Conductive & Ultrasensitive Pattern for Identifying Slow, Fast, Weak and Strong Human Motions at Diverse Conditions

Received 00th January 20xx,
Accepted 00th January 20xx

DOI: 10.1039/x0xx00000x

www.rsc.org/

Supriya Das,[a, ¥] Rajan Singh,[b, ¥] Avijit Das,[a,¥] Sudipta Bag,[a] Roy P. Paily[b,c,d] and Uttam Manna [a,c,d]**

The conversion of mechanical deformation into electrical signals is a widely used principle for various relevant applications. Facile & scalable fabrication, ultrahigh-sensitivity, low-response time and uninterrupted performance at severe conditions are hallmarks of an efficient strain-sensor that would be suitable for realistic application. In the past, various approaches were introduced to achieve high gauge factor—mainly associating a large tensile deformation. But, in reality, a flexible strain sensor that displays a high gauge factor at low applied strain and remains efficient to perform at practically relevant diverse and challenging conditions would be more appropriate for unambiguous and effective monitoring of human motions and other relevant applications. But, a low-strain sensor with ultrahigh sensitivity and durability is yet to be introduced in the literature. Here, a metal-free, chemically reactive and conductive ink is unprecedentedly introduced following a 1,4-conjugate addition reaction. Further, a strategic integration of a chemically reactive porous paper with the prepared conductive ink allowed to develop a chemically reactive and conductive interface that allowed desired post covalent modification with selected alkylamines at ambient condition. Taking advantages of spatially selective deposition of prepared ink on chemically recative paper and the ability of post covalent modification of the prepared ink, an abrasion tolerant superhydrophobic & conductive patterned interface was developed for achieving a low-strain (below 0.2%) based flexible strain sensor with an ultrahigh sensitivity (gauge factor ~18,300) and low response time (8 ms). The external low-strain induced cracks on the flexible & durable superhydrophobic and conductive patterned interface provided a facile basis for real-time & wireless monitoring of slow, fast, weak and strong human motions & expressions—at diverse conditions, including continuous aqueous exposures, physical abrasions etc.

Introduction

The conversion of mechanical deformation into an electrical signal in the form of voltage, resistance etc. remained a facile basis for developing different functional materials.[1-5] In this context, different nanomaterials are strategically associated to achieve conductive flexible/stretchable interfaces having organized and complex topography for wide range of potential applications—including wireless monitoring of human motion, soft robotics, electronic skin, etc.[6-15] The desired requisites of an efficient strain sensor that would be appropriate for practical application are a) high sensitivity (means high gauge factor), b) low response time and c) ability to perform at practically relevant challenging settings. In the past, various metal and other conductive nanomaterials were associated following some complex deposition process to achieve strain sensor—but only stretchable strain sensors displayed high gauge factor on incurring a large tensile deformation.[6-15] In reality, the repetitive and large tensile deformation is known to lead an unwanted fatigue & failure in polymeric and soft materials.[16] Further, the attachment of highly stretchable interface with the human skin at different and relevant part of the body demands special and additional arrangements for

[a] *Department of Chemistry, Indian Institute of Technology-Guwahati, Kamrup, Assam 781039, India*
[b] *Department of Electronics and Electrical Engineering, Indian Institute of Technology-Guwahati, Kamrup, Assam 781039, India.*
[c] *Centre for Nanotechnology, Indian Institute of Technology-Guwahati, Kamrup, Assam 781039, India*
[d] *School of Healthcare Science & Technology , Indian Institute of Technology-Guwahati, Kamrup, Assam 781039, India*
¥ indicates equal contribution
E-mail: umanna@iitg.ac.in, roypaily@iitg.ac.in

Electronic Supplementary Information (ESI) available: [The attached supporting information accounting materials and methods, synthesis of AGO, preparation of chemically reactive ink, fabrication of superhydrophobic and conductive patterned interface, Table S1 and Figure S1 to Figure S20 illustrating the performance of strain sensors, finger wiping test, FTIR of APTMS, impact of concentration of AGO on resistance, depostion of chemically reactive conductive ink and its post modifications, physical abrasion tests on superhydrophobic & conductive interfaces, tolerance under different aqueous exposures, stability of the interface at different temperature and humidity, changes in the number of cracks andtheir width, coating on different substrates, estimation of response and recovery time, changes of resistance with the dynamic change of applied strain, hysteresis of signal, reusability of pattern interface, detection of coughing and uttering, monitoring neck bending, monitoring localized.] See DOI: 10.1039/x0xx00000x

achieving desired and unambiguous results.[17] On the other side, the conductive hydrogels are another important class of materials that allowed to develop stretchable strain sensors with high sensitivity and wide detection range. But, the hydrogels can be readily deformed and remained highly sensitive to relative humidity of the environments. In fact, such materials are inadequate to sustain harsh physical and chemically complex aqueous exposures.[18-20] Hence, the design of a flexible sensor with a high gauge factor that performed at low applied strain (below 0.5%) would be a more appropriate approach for various relevant applications. Nevertheless, in the recent past, a few important designs were introduced to report strain sensor with improved sensitivity, linearity, response time, stability, detection limits—following relatively simple fabrication process (see Table S1).[21-26] Unfortunately, the report of extremely water repellent and abrasion tolerant low-strain based sensors with ultrahigh gauge factor is yet to be introduced in the literature as shown in table S1. In our current design, a flexible, non-stretchable and environmentally friendly substrate was extended to design a low strain based (below 0.5%) and non-stretchable motion sensor with high sensitivity.

At realistic settings, a strain sensor is likely to face severe abrasive and complex aqueous exposures—but the tolerance of reported strain sensors towards both the physical and chemical challenges is barely examined in the past.[6-15] Recently, the association of extreme water repellency with strain sensor emerged as an effective approach for preventing unwanted perturbation of electrical signal during the exposures of practically relevant complex & common aqueous conditions.[27-34] In this context, most of the reported conductive superhydrophobic interfaces were derived from environmental hazard and fluorinated molecules,[27-30] moreover barely any reported approach demonstrated the tolerance of prepared superhydrophobic conductive interface under severe abrasive condition[27-34]—which is extremely important for its realistic application. In this communication, we have introduced a

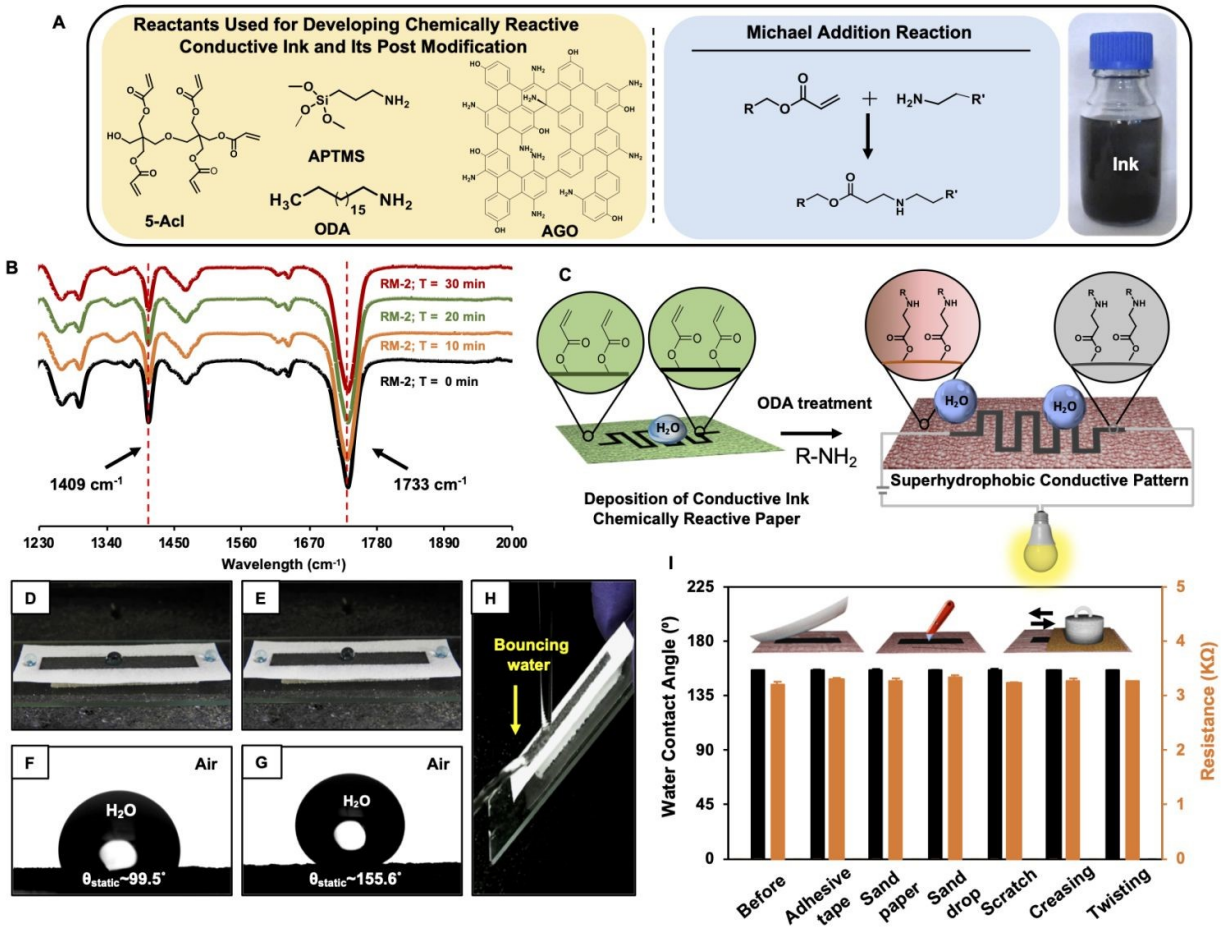

Fig.1 (A) Chemical structures of reactants used for the preparation of a chemically reactive & conductive ink, i.e., dipentaerythritol pentaacrylate (5-Acl), 3-aminopropyltrimethoxysilane (APTMS), octadecylamine (ODA) and aminographeneoxide (AGO); schematic of 1,4-conjugate addition reaction between the acrylate and primary amine groups of the reactants at ambient conditions, without any aid of catalyst. (B) FTIR spectra accounting the 1,4 conjugate addition reaction between amine and acrylate groups in the reaction mixture of 5-Acl, APTMS and AGO, where the IR signature at 1409 cm^{-1} for acrylate group was recorded at different intervals of time. (C) Schematic depicting the fabrication of extremely water repellent & conductive pattern interface, where the chemically reactive conductive ink was deposited spatially selectively on the dip coated chemically reactive paper, prior to post-modify with octadecyl amine (ODA). (D-G) Digital images and static contact angle images of the beaded water droplets on the chemically reactive & conductive interface before (D, F) and after ODA treatment (E, G). (H) Digital image of the bouncing of liquid water after hitting the superhydrophobic and conductive interface. (I) Graph accounting the tolerance of both the embedded water wettability and resistance under various harsh and abrasive physical settings.

simple and roust chemical approach to report i) a physical abrasion tolerant, ii) superhydrophobic & iii) low-strain (0.2%) based resistive strain sensor with iv) a ultra-high gauge factor (~18300), v) low (8 ms) response time and vi) high stability (15000 cycles) for v) real time and wireless monitoring of different human motions/expressions—even in the presence of continuous aqueous exposure.

Results and Discussions

In our current design, 1,4-conjugate addition reaction that appeared as an important avenue for developing various functional & smart materials, [35-37] has extended for achieving a chemically reactive and conductive ink as shown in Figure 1A through the strategic association of selected three distinct reactants (dipentaerythritol pentaacrylate (5Acl, multifunctional crosslinker), aminopropyl trimethoxysilane (APTMS; binder) and amino-graphene oxide (AGO (7% of nitrogen) was prepared following previously reported protocol[38]) at ambient condition. The reaction mixtures (RM-1&2) that were differently formulated with selected reactants allowed to investigate the role of each reactant towards the designing of durable, conductive and superhydrophobic pattern that would be appropriate for designing a low-strain (less than 0.5 %) based ultrasensitive sensor for convenient monitoring of different and relevant human motions/expressions—even in the presence of continuous aqueous exposure. The individual physical deposition of conductive ingredient i.e. AGO and the reaction mixture-1 (RM-1) of AGO/5Acl on bare paper failed to sustain even the finger wiping test and the resistance significantly changed after the application of such common and mild abrasive exposure as shown in Figure S1A-D. Whereas, the reaction mixture-2 (RM-2) that comprised of AGO/5Acl/APTMS remained efficient to tolerate same finger wiping test (Figure S1E-F)—and no change in resistance was noted as shown in Figure S1G. The physical abrasion tolerance is attributed to the self-polymerization of APTMS (Figure S2) and 1,4-conjugate addition reaction between amine and acrylate. As expected, the association of nonconductive reactants (5Acl/APTMS) with AGO in the RM-2 enhanced the resistance of the deposited ink, however, the gradual increment in the content of AGO (from 10 mg/ml to 100 mg/ml) in the reaction mixture helped in lowering the resistance from 102 KΩ to 3.2 KΩ as shown in Figure S3. This particular conductive ink (with resistance of 3.2 KΩ and thickness ~ 30 µm) that derived from reaction RM-2 was selected for the rest of the study.

On the other hand, another reactant i.e. 5Acl a) allowed to covalently integrate the selected conductive material i.e. AGO, and also b) provide essential residual chemically reactivity enabled the deposited conductive ink for appropriate post covalent modifications—following a facile 1,4-conjugate addition reaction between amine and acrylate at ambient condition. The existence of residual acrylate groups in the deposited ink was validated through an attenuated total reflection Fourier-transform infrared spectroscopy (ATR-FTIR) study. The characteristic IR peak intensity for the asymmetric C-H stretching of vinyl moiety of acrylate groups at 1409 cm^{-1} was depleted by ~26 % in the RM-2 over 30 minutes as shown in Figure 1B. No further change in IR peak intensity at 1409 cm^{-1} was noted even after 12 h. The residual acrylate groups in the reaction mixture allowed the post-covalent modification of the deposited and dry ink with selected alkylamine having a long hydrocarbon tail. The subsequent post covalent modification of the deposited ink (that derived from RM-2) on a printer paper with the selected octadecylamine (ODA) altered the water wettability significantly from ~89.2° to 142° as shown in Figure S4. The post covalent modification of the deposited ink was further characterized through the ATR-FTIR study. The signature for the residual acrylate group at 1408 cm^{-1} was significantly diminished after the post covalent modification of the conductive ink with ODA as shown in Figure S5. Thus, a chemically reactive and conductive interface (with resistance of 3.2 KΩ) is developed through the strategic use of 1,4-conjugate addition reaction at ambient conditions. During this post covalent modification process, the change in resistance of the deposited ink was not observed. Thereafter, a superhydrophobic and conductive pattern (Figure 1C) was developed by strategic association of this amine-reactive and conductive ink (CRCI) with a chemically reactive paper—was prepared by dip-coating a selected paper into a dispersion of chemically reactive polymeric nanocomplex—following the earlier reported protocol.[39] The post covalent modification of deposited CRCI (WCA~ 99°, Figure 1 D,F) on the chemically reactive paper with octadecylamine provided extremely water repellent (WCA of 155°, Figure 1E, G) and conductive (with resistance of 3.2 KΩ) interface, where a stream of water can easily bounce on the extremely water repellent conductive interface as shown in Figure 1H. Such an interface remained efficient to tolerate different and severe abrasive exposures—including twisting, creasing, scratching, adhesive tape test, sandpaper abrasion test, sand drop test as shown in Figure 1I and Movie 1-3. Both the water wettability and the resistance remained mostly unaffected after exposing the superhydrophobic and conductive interface to such practically relevant and challenging conditions as shown in Figure 1I and Figure S6. Thereafter, the deposited chemically reactive ink before and after post covalent modifications with ODA were separately exposed to different aqueous phases to examine the impact of the embedded superhydrophobicity on the resistance of the conductive interface. While, different aqueous phases easily infiltrated into chemically reactive ink and altered the resistance of the conductive interface, the embedded superhydrophobicity prevented infiltration of aqueous phase—and the resistance of the same conductive interface after ODA modification remained unaffected as shown in Figure S7. Moreover, a negligible change in the electrical performance (resistance) was observed on the exposure of the prepared conductive interface to a broad range of temperature (from 0°C to 70°C) and relative humidity (from 1% to 90%) as shown in Figure S8.

View Article Online
DOI: 10.1039/D1MH01071A

The flexible, conductive (with resistance of 3.2 KΩ and thickness ~ 30 µm) and superhydrophobic (static WCA ~155°, Figure 1E, G) interface (denoted as FCSI) was further extended to examine its ability towards strain sensing performance. The resistance of the superhydrophobic and conductive interface readily and reversibly changed from 3.2 KΩ to 25.6 KΩ on bending the selected substrate with 30° as shown in Figure 2A-C. After releasing the applied bending, the substrate returned to its initial shape and the resistance of the conductive interface was restored back to 3.2 KΩ (Figure 2C). On bending, the hierarchically featured interface where AGO were randomly oriented as examined with the FESEM study in Figure 2E. On bending the ink deposited flexible substrate, some microcracks appeared in the same interface (Figure 2F), however, on releasing the applied strain, the microcracks disappeared (Figure 2G). This reversible appearance of cracks supports the switchable change in the resistance of the FCSI. The elevated bending angles influenced both the number of cracks and width of the cracks on the prepared conductive interfaces as shown in Figure S9. Eventually, the resistance of the interface changed

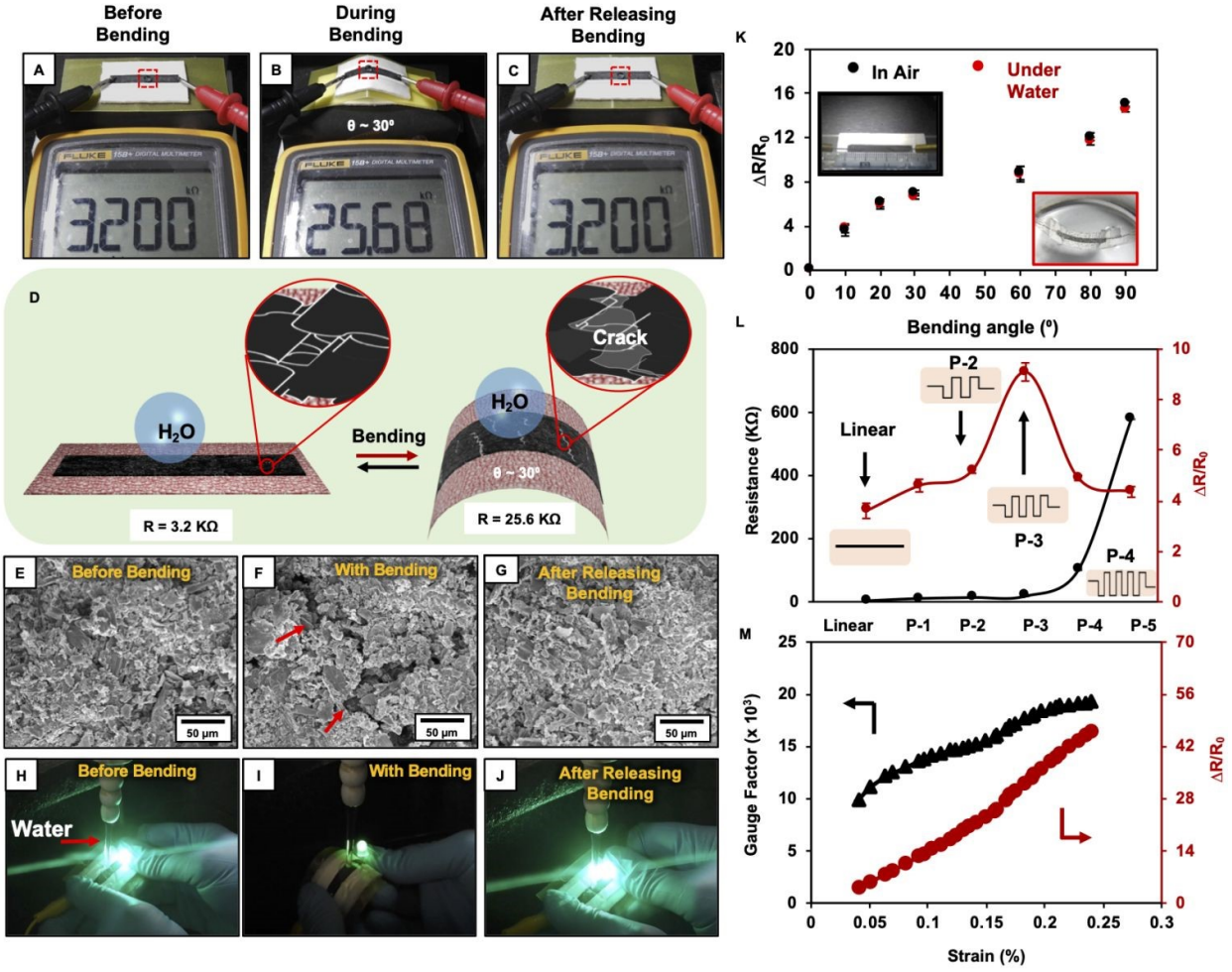

Fig.2 (A-C) Digital images depicting the revisable changes (from 3.2 KΩ to 25.6 KΩ) in the resistance of the superhydrophobic and conductive interface on incurring bending from 0° to 30°. (D) Schematic showing the appearance of reversible cracks during bending of the superhydrophobic and conductive interface. The change in resistance is attributed to this crack on the conductive interface. (E-G) FESEM images revealed the existence of reversible crack during the bending of conductive and superhydrophobic interface. (H-J) Demonstrating the reversible change in the resistance under continuous exposure of aqueous phase, where the brightness of the LED light varied with bending the conductive and superhydrophobic interface under the continuous exposure of aqueous phase (see Movie 4 for more details). (K) The resistance of superhydrophobic and conductive interface enhanced with increasing the bending angle both in air (black) and under submerged (red) condition. L) The plot accounting the absolute resistance and the change in resistance of different water repellent and conductive pattern interfaces (linear, P-1, P-2, P-3, P-4, and P-5, see Figure S9 for more details) on associating identical bending. (M) The graph accounting change in resistance (red) and gauge factor (black) of the optimized pattern (i.e. P-3) interface under different applied strain.

change in the resistance of the deposited ink on the flexible substrate is likely due to the generation of physical cracks and defects as depicted in Figure 2D. In the past, the induction of cracks & defects in a well-organized conductive interface remained a widely used principle to develop strain sensors.[12] However, the deposition of RM-2 provided a with increasing the bending angle. Further, an experiment designed to examine the bending assisted change in resistance of the superhydrophobic and conductive interface—even in the presence of continuous exposure to the tap water. First, the superhydrophobic ink was connected to a commercially available light-emitting diode (LED) using a battery input of 9 V.

Thereafter, the superhydrophobic ink that was kept in the contact with the stream of water was gradually bent as shown in Figure 2H-I and Movie 4. The light intensity of the LED significantly depleted on the application of the manual bending to the FCSI, however, after releasing the applied strain, the light intensity of the LED recovered back as shown in Figure 2J. This simple demonstration confirmed that the developed conductive interface remained efficient to perform— in the presence of continuous water exposure. Furthermore, the change in the resistance of FCSI was examined by increasing the bending angle (from 0° to 90°) both in air and under water. The change in resistance of the FCSI gradually increased from 3.2 KΩ to 15 KΩ as shown in Figure 2K (black), and a very similar result was obtained on repeating the same experiment under water as shown in Figure 2K (red). Thus, the embedded superhydrophobicity allowed FCSI to perform—even under water. The current coating approach can be successfully extended to other flexible substrates—with ability to display similar water repellency (above 150°) and change in resistance as shown in Figure S10.

The prepared conductive ink can be deposited with spatial selectivity on the hydrophobic and chemically reactive paper following different standard processes—including stamp printing and screen printing (Figure S11). By taking advantage of this spatially selective deposition of the conductive ink, different patterned conductive & superhydrophobic interfaces with variable resistance were prepared for developing a strain sensor with high gauge factor—that accounts for the sensitivity of the prepared sensor. The spatially selective deposition of chemically reactive and conductive ink on a chemically reactive paper allowed to prepare patterned interfaces (denoted as P-1, P-2, P-3, P-4 and P-5, Figure 2L) with variable the end to end distance (3 cm to 20.6 cm) of the conductive region—keeping the overall dimension of all the patterns identical, i.e. 3 cm (see Figure S12). With increasing the end to end distance (from 3 cm to 20.6 cm) of the deposited conductive ink, the absolute resistance of the patterned interfaces gradually enhanced from 3.2 KΩ to 578.3 KΩ. Interestingly, the change in the resistance was observed to be maximum (9.1 times) for P-3 (Figure 2L, red line) at identical conditions, where each and every patterned interface were bent at 10°. Thereafter, the sensitivity of P-3 was examined on application of low strain (less than 0.5 %). The gauge factor that accounts sensitivity of the P-3 against the applied strain was calculated following the widely used & standard equation[6]:

$$\text{Gauge Factor (GF)} = (\Delta R/R_0)/\varepsilon \quad \text{.....Eq. 1}$$

Where, R_0 and ΔR are absolute resistance and the change in the resistance of the patterned interface (P-3) after incurring the applied strain (denoted as ε). The applied ε on the patterned (P-3) interface was calculated using Eq. 2 and Eq.3.

$$\varepsilon = (\pm)\ h/2R \quad \text{.....Eq. 2}$$
$$C = 2R \sin(L/2R) \quad \text{.....Eq. 3}$$

Where, h, L, C and R represents the thickness of the sensor (30 μm), the arc length (3 cm), the chord length and the radius of curvature of the synthesized strain sensor. A schematic diagram to illustrate the above mentioned parameters and the change of chord length (L) with radius of curvature (R) are provided in Figure S13. The change of the applied strain on the prepared interface influenced the gauge factor of the sensor—likely due to the difference in the number and width of the generated cracks (see Figure S9). The gauge factor of P-3 was observed to be ~15,800 at very low (0.15%, equivalent to bending at 60°) applied strain. In the past, mostly strain sensors with high GF values were obtained by application of very large tensile strain, however the report of low strain-based sensors with GF value above 1000 is extremely rare to achieve as shown in Table S1. Thus, the current approach of chemically reactive and conductive ink that derived through 1,4 conjugate addition reactions provided a unique solution to achieve a flexible, paper-based and extremely water-repellent conductive pattern with unprecedented gauge factor at low applied strain. Such a principle would be appropriate for monitoring various human motions/expressions and other relevant biomedical and robotic applications.

Apart from the gauge factor, a rapid response of conductive interface towards applied strain and fast recovery of the change in resistance after releasing the applied strain are other key characteristics of an efficient strain sensor. The superhydrophobic and conductive pattern (P-3) interface was bent at 30° and monitored both the change and recovery of the resistance with time as shown in Figure S14. Interestingly, the currently developed interface provided a rapid response (8 ms) to the applied strain and a very fast recovery (21 ms) was noted after releasing the applied strain as shown in Figure S14. Such rapid response to applied strain is rare in the reported sensors as discussed in the Table S1. The change in the resistance of the prepared sensor was noticed to be gradually altered with the association of dynamic change in the applied strain (i.e. increment/decrement of bending deformations) as shown in Figure S15. Moreover, the change in the resistance due to the bending of the interface was observed to be completely reversible as confirmed from the hysteresis curve in Figure S16. Further, the pattern interface was repetitively bent at 30° using am automated mechanical device (Movie 5) for 15,000 times, and the change in the resistance of the same interface was measured with bending angle of 30° at regular interval as presented in Figure S17A. Further, the change in the resistance at each and every step during the process of incurring the bending of 30° for 1000 times is also provided in Figure S11B. But, the change in the resistance remained unaltered after successive bending of the flexible interface. Such repetitive performance, rapid response and fast recovery of the synthesized strain sensor (P-3) attributed to the design of unique chemically reactive and conductive ink, where the covalently crosslinked and hierarchically featured network of AGO remained chemically reactive for associating desired superhydrophobicity and random hierarchical feature is likely to contribute towards the crack induced reversible & rapid change in the resistance with fast recovery time.

View Article Online
DOI: 10.1039/D1MH01071A

Thereafter, the extremely water repellent and conductive pattern (P-3) was associated with both the Arduino Nano board (version 3) and the Bluetooth module HC-05 for wireless prepared patterned interface in air was demonstrated with the help of the display of a smartphone as illustrated in the Movie 6. Next, the same pattern interface was gradually bent

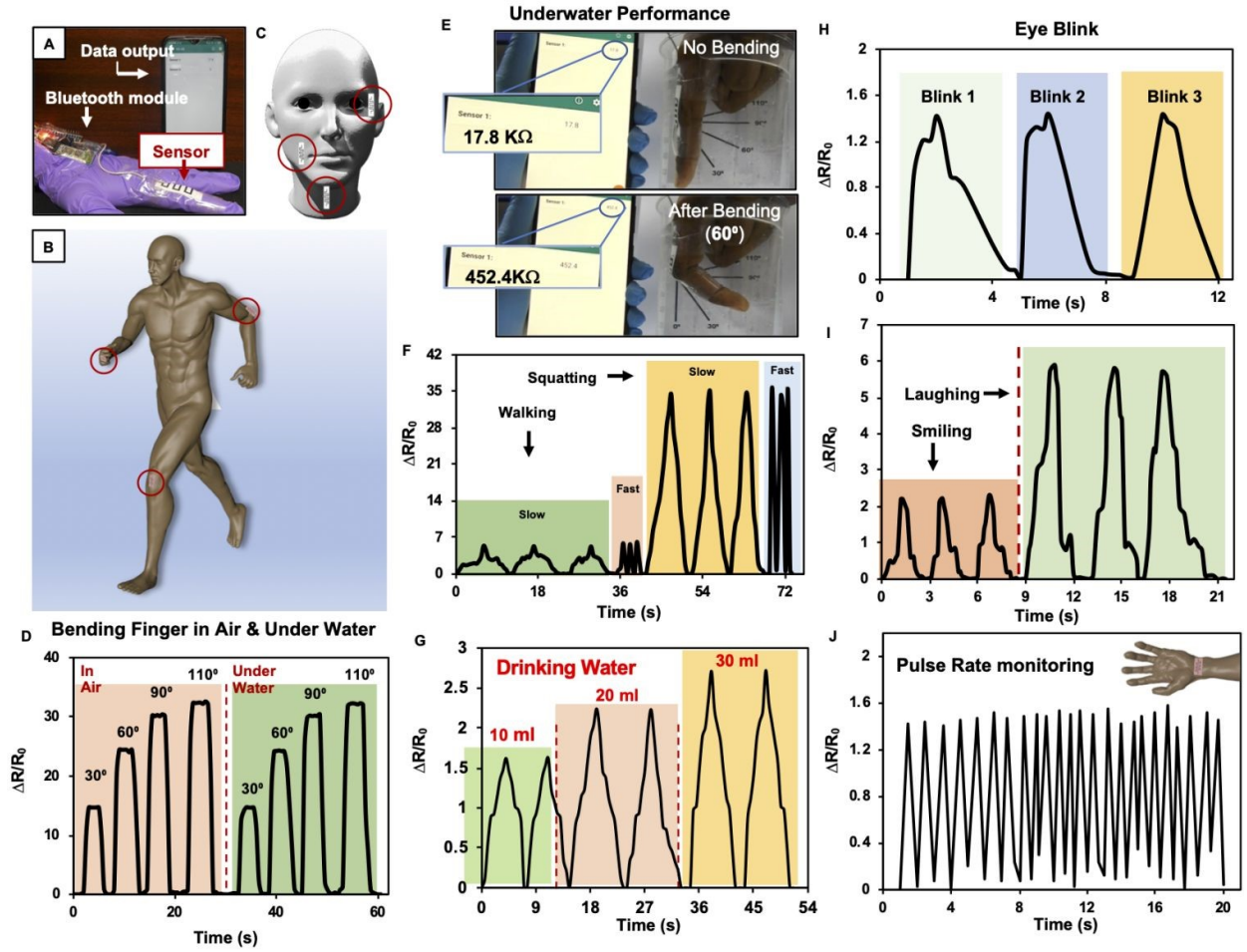

Fig. 3 (A) Digital image showing the set-up consisting of sensor, Bluetooth module and data output device (e.g. smart phone) for wireless detection of different motions (B) and expressions (C) of human, where the superhydrophobic and conductive pattern (P-3) interface was used as sensor and appropriate attachment of this pattern interface allowed to monitor different motions and expressions, where red circle pointing out the position of sensor (pattern interface: P-3). (D) The plot accounting the gradual change in resistance of pattern interface that attached to a finger of a volunteer on bending the finger at different angles (from 30° to 110°) both in air (left side) and under water (right side). E) Digital images displaying the instant change of resistance (from 17.8 KΩ to 452.4KΩ) after incurring the bending of 60° of the superhydrophobic and conductive patterned interface underwater (see movie 7). F-J) Plots illustrated the electrical response (in form of change in resistance) of the superhydrophobic and conductive pattern (P-3) interface that attached to different part of a volunteers' body (C-D) for monitor walking & squatting (F), swallowing of drinking water with different volumes (G), bilking of eye (H), smiling & laughing (I) and wrist pulse rate (J). See movie 8 for more details.

monitoring of different human motions and expressions as illustrated in Figure 3A. The adequate attachment of patterned interface (P-3) at appropriate location is essential to achieve characteristic signal (i.e. change in resistance) during both soft and strong movement of different parts (elbow, knee, finger, throat, neck eyes etc.) of the human body as depicted in Figure 3B-C. As a proof of concept demonstration of wireless detection of different soft and strong human motions, the patterned interface (P-3) was first attached on a finger prior to bend at different angles, the change in the resistance was noted to be gradually elevated with increasing the bending angle—from 30° to 110° in air as depicted in Figure 3D. A real-time and wireless change in the resistance during the bending of the underwater as depicted in Figure 3E—and a very similar change in resistance was noted as shown in Figure 3D (right side: green shaded area) and Movie 7. As expected, the embedded superhydrophobicity allowed the successful underwater performance of the conductive pattern interface.

Later, the same conductive pattern interface was attached to the knee of an adult volunteer from our lab for monitoring both slow (~5 steps/minute) and fast (~30 steps/minute) walking, where the nature of resistance changes was noticed to be very different depending on the speed of the walking. Due to the slower bending of the knee, the base width of the signal (change in resistance vs time) was noticed to be large, in comparison to

View Article Online DOI: 10.1039/D1MH01071J

the fast walking. As expected, the amplitude of the change in resistance remained very similar as the extent of bending of the knee kept merely the same for both the occasions as shown in Figure 3F. Further, this conductive pattern interface remained efficient to differentiate the walking and squatting movements. A significantly higher (~ 7 fold more) change in resistance was noted during the squatting as it caused more bending of the pattern interface. Again, a completely distinct pattern of the signal (change in resistance vs time) was noted for fast (6/minute) and slow (36/minute) squatting as depicted in Figure 3F. Thereafter, the conductive pattern interface was attached at the throat of a lab volunteer to monitor coughing (Figure S18 A), uttering different words (Figure S18 B) and swallowing of different volumes of water (Figure 3G). As expected, on increasing the volume (from 10 ml to 30 ml) of the drinking water, the amplitude for the change in the resistance is enhanced as shown in Figure 3G. Interestingly, the attached conductive patterned interface on the neck allowed it to detect even forward and backward movement of the neck as shown in Figure S19. The concave (~30°) and convex (~60°) bending of the neck provided two distinct forms of the signal during both forward and backward movements, respectively. Furthermore, the same paper-based superhydrophobic & conductive pattern, i.e. P-3 was attached at the appropriate parts of the face (Figure 3C) for detecting different facial expressions—including blinking of eyes, smiling and laughing as shown in Figure 3 H-I. The blinking of eyes led to a very minute change in the facial deformation—but the prepared ultrasensitive conductive patterned interface remained efficient to detect such facial expressions as depicted in Figure 3H. On the other side, laughing caused more deformation of the face in comparison to smiling resulting in a distinct signal (change in resistance with time) as shown in Figure 3I. During the course of the study, we noticed that a localized pressure on such pattern interfaces can lead to a significant change in resistance. Most likely, the localized load on such flexible interface led to some local deformation—which remained sufficient to perturb the resistance of the patterned interface as depicted in Figure S20A-B. To validate this hypothesis, we have placed water droplets with different volumes on the superhydrophobic & conductive interface, prior to measure the change in resistance. With increasing the volume of beaded water droplets, an elevation of the change in the resistance was noted as shown in Figure S20C. This simple study provided a facile basis to monitor events that are associated with localized pressure. For example, the currently developed pattern interface was extended to monitor pulse rate that is associated with a weak and localized mussel movement. Interestingly, the attachment of the pattern interface (P-3) at the wrist of an adult male, allowed to successfully monitor the wrist pulses as shown in Figure 3J and Movie 8, where 24 significant spikes appeared within 20 seconds—due to the successive change of resistance.

Conclusion

In conclusion, an extremely water-repellent and abrasion tolerant conductive pattern interface is unprecedentedly and successfully introduced for low-strain based ultra-sensitive detection of both strong and weak movements of body parts during walking, squatting, coughing, uttering, swallowing, blinking, wrist pulses etc. Thus, such an approach could be extremely useful in studying the interaction of human/machine and monitoring patients during the rehabilitation process. Further, the embedded water repellency and ability to sustain severe abrasive exposure allowed it to perform under water and at various practically relevant extremes of conditions. Thus, the current and simple design of superhydrophobic and conductive pattern interface has immense potential for different and more realistic applications.

Conflicts of interest:

There are no conflicts to declare.

Acknowledgements

The financial support of Science and Engineering Research Board (CVD/2020/000018), Government of India is well-acknowledge. We thank CIF, Centre for Nanotechnology and Department of Chemistry, School of Health Science & Technology, Indian Institute of Technology-Guwahati, for their kind support in executing various experiments and for the infrastructures. We also thanful to Mr. Akshay Namdeo for his kind help and suggestions. Mr. Avijit Das and Mr. Sudipta Bag are grateful to CSIR for their SRF and JRF fellowships. Ms. Supriya Das and Rajan Singh thank MoE and IIT G for their PhD fellowships. Dedicated to Prof. Arun Chattopadhyay, FNA, J C Bose Fellow

References

1. C. Wang, D. Hwang, Z. Yu, K. Takei, J. Park, T. Chen, B. Ma and A. Javey, *Nature Materials,* 2013, **12**, 899.
2. M. Amjadi, K. U. Kyung, I. Park and M. Sitti, *Adv. Funct. Mater.,* 2016, **26**, 1678.
3. W. Liu, M.-S. Song, B. Kong and Y. Cui, *Adv. Mater.,* 2017, **29**, 1603436.
4. G. J. N. Wang, A. Gasperini and Z. Bao, *Adv. Electron. Mater.,* 2018, **4**,1700429.
5. M. Amit, L. Chukoskie, A. J. Skalsky, H. Garudadri and T. N. Ng, *Adv. unct. Mater.*, 2020, **30**, 1905241.
6. Z. Liu, D. Qi, P. Guo, Y. Liu, B. Zhu, H. Yang, Y. Liu, B. Li, C. Zhang, J. Yu, B. Liedberg and X. Chen, *Adv. Mater.,* 2015, **27**, 6230.
7. S. Chen, Y. Song, D. Ding, Z. Ling and F. Xu, *Adv. Funct. Mater.,* 2018, **28**, 1802547.
8. F. Sun, M. Tian, X. Sun, T. Xu, X. Liu, S. Zhu, X. Zhang and L. Qu, *Nano Lett.,* 2019, **19**, 6592.
9. X. Shi, S. Liu, Y. Sun, J. Liang and Y. Chen, *Adv. Funct. Mater.,* 2018, **28**, 1800850.
10. Y. Qiao, Y. Wang, H. Tian, M. Li, J. Jian, Y. Wei, Y. Tian, D.-Y. Wang, Y. Pang, X. Geng, X. Wang, Y. Zhao, H. Wang, N. Deng, M. Jian, Y. Zhang, R. Liang, Y. Yang and T.- L. Ren, *ACS Nano,* 2018, **12**, 8839.
11. K.-H. Kim, N.-S. Jang, S.-H. Ha, J. H. Cho and J.-M. Kim, *Small,* 2018, **14**, 1704232.

View Article Online
DOI: 10.1039/D1MH01071A

12. W. Miao, Y. Yao, Z. Zhang, C. Ma, S. Li, J. Tang, H. Liu, Z. Liu, D. Wang, M. A. Camburn, J.-C. Fang, R. Hao, X. Fang, S. Zheng, N. Hu and X. Wang, *Nature Communication,* 2019, **10**, 3862.
13. Y. Yanga, Z. Caoa, P. Hed, L. Shia, G. Dingd, R. Wanga and J. Sun, *Nano Energy*, 2019, **66**, 104134.
14. C. Tan, Z. Dong, Y. Li, H. Zhao, X. Huang, Z. Zhou, J.-W. Jiang, Y.-Z. Long, P. Jiang, T.-Y. Zhang and B. Sun, *Nature Communication,* 2020, **11**, 3530.
15. C.-Z. Hang, X.-F. Zhao, S.-Y. Xi, Y.-H. Shang, K.-P. Yuan, F. Yang, Q-G. Wang, J-C. Wang, D. W. Zhang and H.-L. Lu, *Nano Energy,* 2020, **76**, 105064.
16. Z. Wang, C. Xianga, X. Yaoa, P. L. Flocha, J. Mendeza and Z. Suo, *Proceedings of the National Academy of Sciences of the United States of America,* 2019, **116**, 5967.
17. S. Wang, Y. Fang, H. He, L. Zhang, C. Li and J. Ouyang, *Adv. Funct. Mater.,* 2021, **31**, 2007495.
18. Z. Wu, X. Yang and J. Wu, *ACS Appl. Mater. Interfaces* 2021, **13**, 2128.
19. J. Wu, Z. Wu, X. Lu, S. Han, B.-R. Yang, X. Gui, K. Tao, J. Miao and C. Liu, *ACS Appl. Mater. Interfaces* 2019, **11**, 9405.
20. Z. Wu, W. Shi, H. Ding, B. Zhong, W. Huang, Y. Zhou, X. Gui, X. Xie and J. Wu, *Journal of Materials Chemistry C*, 2021, DOI: 10.1039/D1TC02506F.
21. M. Amjadi, M. Turan. M, P. C. Clementson and S. Metin, *ACS Appl. Mater. Interfaces* 2016, **8**, 5618.
22. X. Fang, J. Tan, Y. Gao, Y. Lu and F. Xuan, *Nanoscale*, 2017, **9**, 17948.
23. J. Lee, S. Shin, S. Lee, J. Song, S. Kang, H. Han, S. G. Kim, S. Kim, J. Seo, D. E. Kim and T. Lee, *ACS Nano* 2018, **12**, 4259.
24. N. Gupta, K. D. M. Rao, K. Srivastava, R. Gupta, A. Kumar, A. Marconnet, T. S. Fisher and G. U. Kulkarni, *ACS Appl. Mater. Interfaces* 2018, **10**, 44126−44133.
25. F. Yin, J. Yang, P. Ji, H. Peng, Y. Tang and W. Yuan, *ACS Appl. Mater. Interfaces* 2019, **11**, 18645−18653.
26. Y. Gao, Q. Li, R. Wu, J. Sha, Y. Lu, and F. Xuan, *Adv. Funct. Mater.* 2019, **29**, 1806786-1806795.
27. J. Lin, X. Cai, Z. Liu, N. Liu, M. Xie, B. Zhou, H. Wang and Z. Guo, *Adv. Funct. Mater.,* 2020, **30**, 2000398.
28. J. Gao, L. Wu, Z. Guo, J. Li, C. Xua and H. Xuea, *J. Mater. Chem. C,* 2019, **7**, 4199.
29. J. Gaoa, L. Wanga, Z. Guoa, B. Lia, H. Wanga, J. Luoa, X. Huanga and H. Xuea, *Chemical Engineering Journal,* 2020, **381**, 122778.
30. P. Wang, W. Wei, Z. Li, W. Duan, H. Han and Q. Xie, *J. Mater. Chem. A,* 2020, **8**, 3509.
31. Q. Li, H. Liu, S. Zhang, D. Zhang, X. Liu, Y. He, L. Mi, J. Zhang, C. Liu and C. Shen, *ACS Appl. Mater. Interfaces,* 2019, **11**, 21904.
32. S. Wang, X. Du, Y. Luo, S. Lin, M. Zhou, Z. Du, X. Chenga and H. Wanga, *Chemical Engineering Journal,* 2021, **408**, 127363.
33. Z. Chu, W. Jiao, Y. Huang, Y. Zheng, R. Wang and X. He, *J. Mater. Chem. A,* 2021, **9**, 9634.
34. L. Liu, Z. Jiao, J. Zhang, Y. Wang, C. Zhang, X. Meng, X. Jiang, S. Niu, Z. Han and L. Ren, *ACS Appl. Mater. Interfaces,* 2021, **13**, 1967.
35. U. Baruah and U. Manna, *Chem. Sci.,* 2021, **12**, 2097.
36. C. Liu, H. Bai, B. He, X. He, J. Zhang, C. Chen, Y. Qiu, R. Hu, F. Zhao, Y. Zhang, W. He, J. H. C. Chau, S. Chen, J. W. Y. Lam and B. Z. Tang, *Angew. Chem. Int. Ed.,* 2021, **60**, 2.
37. U. Baruah, U. Manna, *Chem. Sci.* **2021**, *12*, 2097.
38. A. Das, J. Deka, K. Raidongia, U. Manna, *Chem. Mater.* 2017, **29**, 8720.
39. S. Das, A. Das, D. Parbat and U. Manna, *ACS Appl. Mater. Interfaces,* 2019, **11**, 34316.